containing 1 mg/ml BSA, respectively. They were diluted with serum-free culture medium (0.1% as the final DMSO concentration). MBEC4 cells were cultured for 3 days in the three in vitro BBB models. The inserts and wells were washed three times with serum-free medium prior to the experiments. To examine the influence of the inhibition of TGF-β1 signaling on the pericyte-induced changes in BBB functions, SB431542 (10 μM) and monoclonal anti-human TGF-β1 antibody (10 μg/ml; R&D Systems, Minneapolis, MN) were loaded in both compartments of the opposite coculture system. In the MBEC4 monolayer, cells were exposed to 1 ng/ml TGF-β1 injected into the inside (luminal) or outside (abluminal) of the insert for 12 h and subjected to experiments to test whether MBEC4 cells exhibit functional polarity in response to TGF-β1. TGF-β1 and the TGF-β1 receptor antagonist (SB431542) were applied for 12 h to the inside of the insert in the MBEC4 monolayer to investigate the effect of SB431542 on the TGF-β1-induced changes in BBB functions. In all experiments, controls were performed by treating cells with serum-free medium containing the corresponding amount of DMSO and/or 4 mM HCl containing 1 mg/ml BSA as the vehicle.

2.9. Statistical analysis

Values are expressed as the mean ± SEM. Statistical analysis was performed using Student's *t* test. One-way and two-way analyses of variance (ANOVAs) followed by Tukey–Kramer's tests were applied to multiple comparisons. The differences between means were considered to be significant when *P* values were less than 0.05.

3. Results

3.1. BBB functions in three in vitro BBB models and expression of TGF-β1 mRNA in rat pericytes

After MBEC4 cells were cultured for 3 days, the basal permeability and P-gp efflux pump of MBEC4 cells were evaluated in three models of the BBB (Fig. 1). The permeability coefficient of Na-F for MBEC4 cells significantly decreased by 34.8% and 16.0% in the opposite and bottom coculture systems, respectively, when compared to that in the MBEC4 monolayer (Fig. 1A). The accumulation of rhodamine 123 in MBEC4 cells significantly decreased by 17.8 and 7.8% in the opposite and bottom coculture models relative to the MBEC4 monolayer, respectively (Fig. 1B).

To obtain molecular evidence for the expression of TGF-β1 in rat pericytes, RT-PCR was carried out with a primer pair specific for rat TGF-β1 (Fig. 2). RT-PCR with mRNA obtained from rat pericytes yielded a single product. The size of this product was the same as that expected from the primer positions in rat TGF-β1.

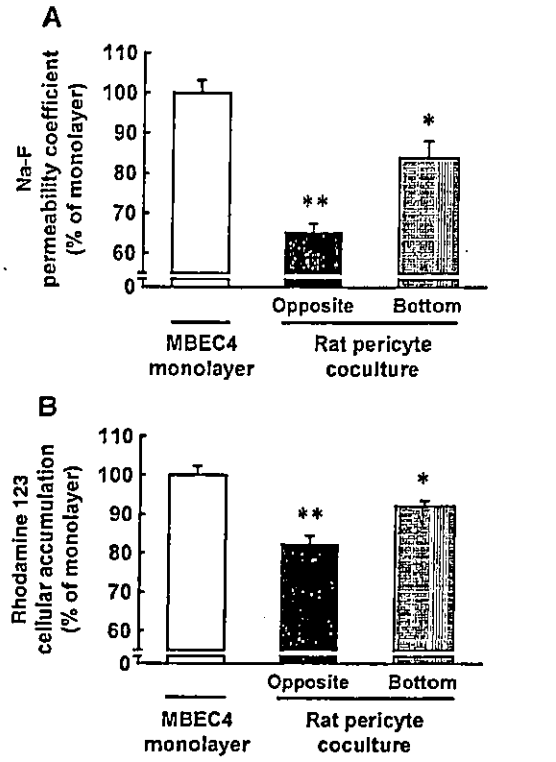

Fig. 1. Permeability and P-gp function of MBEC4 cells in the MBEC4 monolayer and rat pericyte opposite or bottom coculture systems. (A) MBEC4 permeability coefficients of Na-F. Results are expressed relative (%) to the value for the MBEC4 monolayer ($2.7 \pm 0.20 \times 10^{-4}$ cm/min). Values are the means ± SEM (n = 4–12). *P < 0.05, **P < 0.01, significant difference from MBEC4 monolayer. (B) Rhodamine 123 accumulation in MBEC4 cells. Results are expressed relative (%) to the value for the MBEC4 monolayer (1.61 ± 0.25 nmol/mg protein). Values are the mean ± SEM (n = 4–12). **P < 0.01, significant difference from MBEC4 monolayer.

3.2. Effect of the inhibition of TGF-β1 signaling on BBB functions in the MBEC4 monolayer and rat pericyte opposite coculture

As shown in Fig. 3, exposure to anti-TGF-β1 antibody for 12 h inhibited the pericyte-induced enhancement of endothelial barrier and P-gp function in rat pericyte cocultures, whereas anti-TGF-β1 antibody had no significant effect on BBB functions in the MBEC4 monolayer. In the coculture models, anti-TGF-β1 antibody (10 μg/ml) increased the permeability coefficient of Na-F for MBEC4 cells from 86.7 ± 6.1 to 101.7 ± 9.1% of the control value (vehicle-treated MBEC4 monolayer) and the accumulation of rhodamine 123 in MBEC4 cells from 76.6 ± 6.5 to 90.1 ± 8.0% of the control value (Fig. 3). For the permeability to Na-F (Fig. 3A), a two-way ANOVA showed significant effects for the factors culture system (monolayer and coculture) [$F(1, 25) = 4.65$, $P < 0.05$], treatment (vehicle and antibody) [$F(1, 25) = 8.25$, $P < 0.01$] and interaction (culture system × treatment) [$F(1, 25) = 11.51$, $P < 0.005$]. For accumulation of rhodamine 123 (Fig. 3B), a two-way ANOVA showed

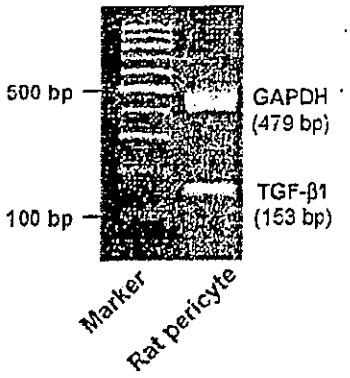

Fig. 2. TGF-β1 mRNA expression in rat pericytes detected by RT-PCR analysis. RNA samples from rat pericytes were used for RT-PCR with primer pairs specific for rat TGF-β1 and GAPDH.

significant effects for culture system [$F(1, 18) = 14.88$, $P < 0.005$] and interaction [$F(1, 18) = 11.97$, $P < 0.005$], but not for treatment. Tukey–Kramer post hoc tests indicated that anti-TGF-β1 antibody significantly increased the permeability to Na-F ($P < 0.01$) and the accumulation of rhodamine 123 in MBEC4 cells ($P < 0.05$) in the coculture system, but not in the monolayer (Fig. 3).

A 12-h exposure to SB431542 (10 μM) significantly increased the permeability from 73.8 ± 3.4 to 87.6 ± 3.9% and moderately elevated the accumulation of rhodamine 123 in MBEC4 cells from 79.0 ± 8.4 to 91.7 ± 11.6% of the control value in the opposite coculture system (Fig. 4). For permeability to Na-F (Fig. 4A), a two-way ANOVA showed significant effects for the factors culture system [$F(1, 21) = 90.10$, $P < 0.0001$], treatment [$F(1, 21) = 14.21$, $P < 0.005$] and interaction [$F(1, 21) = 6.73$, $P < 0.05$]. For the accumulation of rhodamine 123 (Fig. 4B), a two-way ANOVA showed significant effects for culture system [$F(1, 32) = 13.18$, $P < 0.001$] and interaction [$F(1, 32) = 4.16$, $P < 0.05$], but not for treatment. Tukey–Kramer post hoc tests indicated that SB431542 significantly increased the permeability to Na-F ($P < 0.01$) in the coculture system, but not in the MBEC4 monolayer.

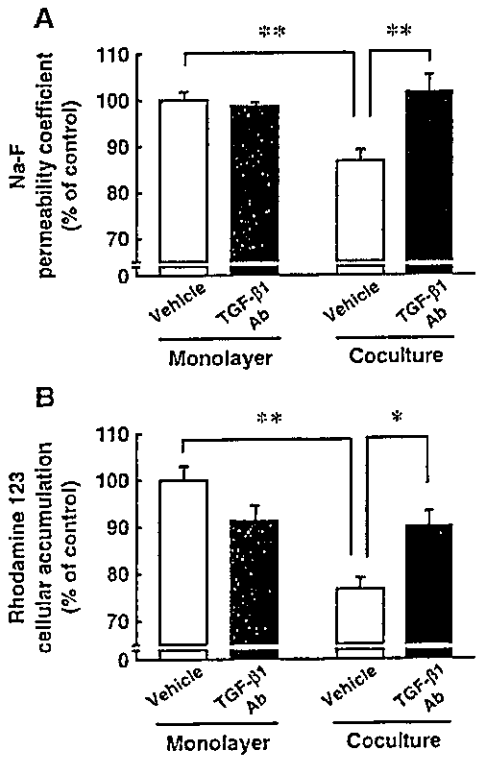

Fig. 3. Effect of anti-TGF-β1 antibody on MBEC4 permeability (A) and P-gp function of MBEC4 cells (B) in the MBEC4 monolayer and rat pericyte coculture systems. Experiments were performed after 12 h of exposure to anti-TGF-β1 antibody (TGF-β1 Ab; 10 μg/ml). (A) MBEC4 permeability coefficients of Na-F. Results are expressed as a percentage of the control (vehicle-treated MBEC4 monolayers) value ($3.85 \pm 0.11 \times 10^{-4}$ cm/min). Values are the means ± SEM ($n = 6$–11). $^{**}P < 0.01$. (B) Rhodamine 123 accumulation in MBEC4 cells. Results are expressed as a percentage of the control value (2.46 ± 0.08 nmol/mg protein). Values are the mean ± SEM ($n = 3$–7). $^{*}P < 0.05$, $^{**}P < 0.01$.

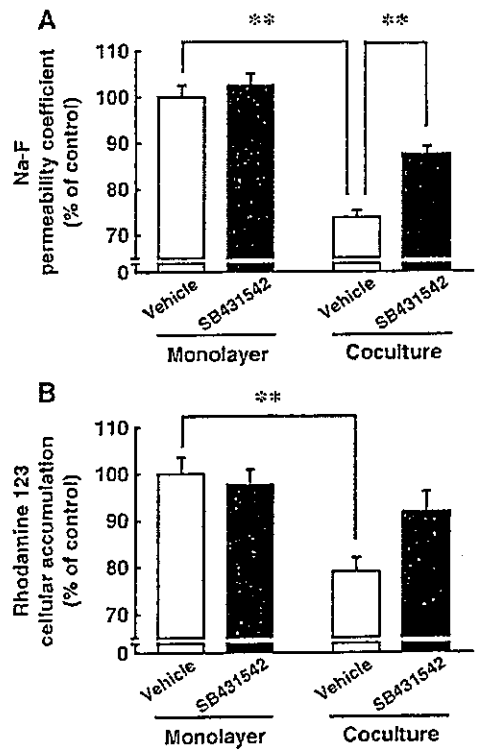

Fig. 4. Effect of a TGF-β type I receptor inhibitor (SB431542) on MBEC4 permeability (A) and P-gp function of MBEC4 cells (B) in the MBEC4 monolayer and rat pericyte coculture systems. Experiments were performed after 12 h of exposure to SB431542 (10 μM). (A) MBEC4 permeability coefficients of Na-F. Results are expressed as a percentage of the control (vehicle-treated MBEC4 monolayers) value ($4.29 \pm 0.18 \times 10^{-4}$ cm/min). Values are the means ± SEM ($n = 4$–8). $^{**}P < 0.01$. (B) Rhodamine 123 accumulation in MBEC4 cells. Results are expressed as a percentage of the control value (2.22 ± 0.43 nmol/mg protein). Values are the mean ± SEM ($n = 7$–12). $^{**}P < 0.01$.

3.3. Effect of TGF-β type I receptor antagonist on TGF-β1-induced enhancement of BBB functions in MBEC4 monolayer

To determine whether the site of treatment had an effect on the permeability of MBEC4 cells, TGF-β1 (10 ng/ml) was applied to the luminal or abluminal side of the MBEC4 monolayer. A 12-h exposure to TGF-β1, when injected into either the luminal or abluminal side, produced significant decreases with the same change in permeability to Na-F (35.7 and 36.6%, respectively) (Fig. 5). Then, TGF-β1 and the TGF-β1 receptor antagonist were applied to the luminal compartment of the MBEC4 monolayer.

The TGF-β1 antagonist SB431542 (10 μM) alone had no effect on the permeability to Na-F and the accumulation of rhodamine 123 in the MBEC4 monolayer. TGF-β1 (1 ng/ml) significantly decreased the permeability ($P < 0.01$ vs. vehicle) and accumulation of rhodamine 123 in MBEC4 cells ($P < 0.01$ vs. vehicle). SB431542 (10 μM) completely blocked the TGF-β1-induced decreases in permeability (106.5 ± 2.2% of vehicle, $P < 0.01$ vs. TGF-β1) and accumulation of rhodamine 123 (107.4 ± 4.0% of vehicle, $P < 0.01$ vs. TGF-β1) (Fig. 6).

4. Discussion

The present study demonstrated that pericytes positively retain BBB functioning through contact with brain endothelial cells and a soluble factor secreted from pericytes. We made three in vitro BBB models; the MBEC4 monolayer, rat pericyte coculture (bottom) and rat pericyte coculture (opposite) (Fig. 1). The pericyte-released substances are permitted to interact with brain endothelial cells through the pores of the insert (0.4 μm pore size) in the bottom coculture model. The opposite coculture model produces a partial contact effect in addition to the soluble factor from pericytes. In the presence of rat pericytes, the permeability to Na-F and the accumulation of rhodamine 123 in MBEC4 cells were markedly decreased (Fig. 1). A positive role for

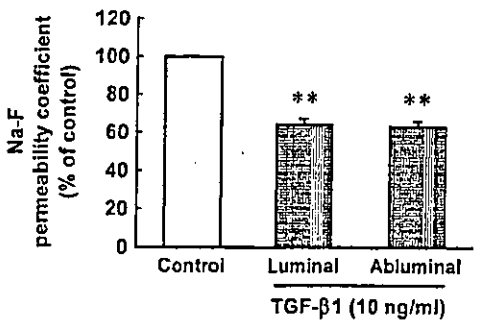

Fig. 5. Functional polarity to the permeability effect of TGF-β1 in MBEC4 monolayers. MBEC4 monolayers were exposed to TGF-β1 (10 ng/ml, 12 h) on either the luminal or abluminal side. The permeability coefficient of Na-F for the control was 2.51 ± 0.02 × 10^{-4} cm/min. Values are the mean ± SEM ($n = 4$). **$P < 0.01$, significant difference from control.

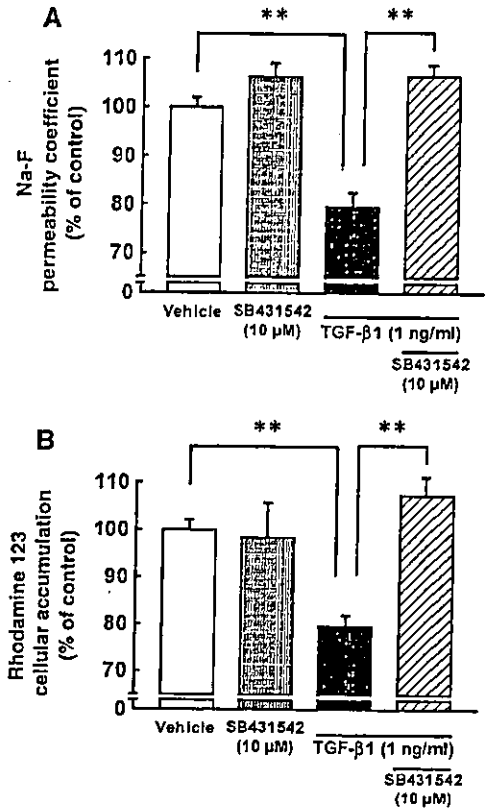

Fig. 6. Effect of a TGF-β type I receptor inhibitor (SB431542) on TGF-β1-enhanced tightening of paracellular junctions (A) and P-gp function of MBEC4 cells (B) in MBEC4 monolayers. Experiments were performed after 12 h of exposure to TGF-β1 (1 ng/ml) and/or SB431542 (10 μM). (A) MBEC4 permeability coefficients of Na-F. Results are expressed as a percentage of the control value (3.66 ± 0.25 × 10^{-4} cm/min). Values are the mean ± SEM (n = 8–12). **$P < 0.01$. (B) Rhodamine 123 accumulation in MBEC4 cells. Results are expressed as a percentage of the control value (1.14 ± 0.02 nmol/mg protein). Values are the mean ± SEM (n = 3–4). **$P < 0.01$.

pericytes in the expression and maintenance of endothelial tight junctions has been documented [13,15], although there are few reports concerning pericyte-enhanced P-gp function. Pericytes in the opposite coculture system apparently enhanced BBB properties compared to those in the bottom coculture model (Fig. 1). These findings suggest that pericytes participate in tightening the intercellular junctions and facilitating P-gp function in brain endothelial cells through the production of soluble factors and cell-to-cell contact. Therefore, we employed the opposite coculture model to investigate effects of the inhibition of TGF-β1 signaling on BBB functions in rat pericyte cocultures.

The anti-TGF-β1 antibody and TGF-β1 receptor antagonist (SB431542) were used here at the maximal concentration having no significant effect on BBB functions in the MBEC4 monolayer. Anti-TGF-β1 antibody reversed the decrease in permeability to Na-F and in the accumulation of rhodamine 123 in the rat pericyte coculture to the corresponding levels in the MBEC4 monolayer (Fig. 3). TGF-β1 receptor antagonist (SB431542) inhibited pericyte-

induced decreases in the permeability to Na-F and the accumulation of rhodamine 123 in MBEC4 cells by 50–60% (Fig. 4). A longer period of exposure than 12 h and/or an injection before 3 days may need to be tested. The present results suggest that the pericyte-induced enhancement of BBB functions is mediated to some extent by TGF-β1. RT-PCR analysis of rat pericytes demonstrated the expression of TGF-β1 (Fig. 2). It is, therefore, conceivable that pericyte-derived soluble factors include TGF-β1 and enhance both tight junctions and P-gp function through, at least in part, the TGF-β type I receptor. This notion is supported by our previous findings that TGF-β1 actually lowers the endothelial permeability and enhances the functional activity of P-gp [8]. In the present study, effects of TGF-β1 adsorption and TGF-β receptor inhibition emerged within 12 h (Figs. 3 and 4), after brain pericytes had induced a restoration of the BBB properties of MBEC4 cells. Thus, brain pericytes seem to positively maintain BBB functioning by continuously producing TGF-β1.

TGF-β expresses its physiological actions predominantly through two types of receptors with serine/threonine kinase activity, TGF-β type I and II receptors [20]. The binding of TGF-β to the TGF-β type II receptor induces the assembly of the TGF-β type I receptor-type II receptor heterodimer, leading to phosphorylation of TGF-β type I induced by the type II receptor. As shown in Fig. 6, SB431542 (10 μM) significantly inhibited the TGF-β1-induced enhancement of BBB functions in the MBEC4 monolayer, suggesting that TGF-β1 facilitates the barrier function of the BBB through the TGF-β type I receptor. It is, therefore, likely that the activation of the TGF-β1/TGF-β receptor pathway between brain endothelial cells and brain pericytes contributes to an enhancement of the tight junctions and P-gp function. Mouse brain capillary endothelial cells expressed TGF-β type I and II receptors [9]. The TGF-β type I receptor was expressed on blood vessels of the basal surface of endothelial cells [9]. In the present study, the enhancement of the permeability and P-gp function of MBEC4 cells induced by TGF-β1 (10 ng/ml) was not dependent on addition to the luminal (blood) or the abluminal (brain) side (Fig. 5). These findings suggest that the TGF-β receptor may be located on both sides of MBEC4 cells. The possibility that TGF-β1 injected into the abluminal compartment is transported in the luminal side through MBEC4 cells could not be excluded. The TGF-β signaling cascades from membrane to nucleus including MAPK and a receptor serine/threonine kinase pathway are probably involved in the enhancement of BBB functions. It is, therefore, conceivable that TGF-β facilitates the barrier function and P-gp functional activity of brain endothelial cells by increasing the expression of tight junction-associated proteins (such as occludin and claudins) and P-gp. The signal molecules involved in the enhancement of BBB functions following the activation of TGF-β1/TGF-β receptor pathway are now under investigation.

In several neurodegenerative diseases, changes in BBB functions and an increase of TGF-β1 in the brain have been described [11,16]. However, it has not been determined whether the increase in the expression of TGF-β observed in human neurodegenerative diseases is the underlying cause or the result of degenerative conditions. Thus, TGF-β1 seems to protect against impairment of the BBB and positively maintain brain homeostasis. In fact, the degeneration of pericytes was observed in neurodegenerative diseases [19,30]. This phenomenon probably decreases TGF-β production, leading to dysfunction of the BBB.

Other soluble factors derived from pericytes, VEGF and bFGF, were reported to influence BBB functions. VEGF increased the permeability of brain endothelial cells, suggesting that VEGF is a barrier-weakening factor [31]. bFGF was found to tighten the intercellular junctions and induce the expression of multidrug resistance proteins [26]. TGF-β1 up-regulated the induction of bFGF production [10]. Angiopoietin-1, an antipermeability factor [18] secreted from pericytes, produced the expression of occludin mRNA in brain endothelial cells [15]. It is, therefore, conceivable that brain pericytes regulate BBB functions by secreting these substances. TGF-β1, VEGF, bFGF and angiopoietin-1 appear to be involved in the interaction of endothelial cells, pericytes and astrocytes under physiological and pathophysiological conditions, since these substances are also produced by astrocytes.

In conclusion, brain pericytes induce and up-regulate the barrier function and P-gp functional activity of brain endothelial cells. This pericyte-induced up-regulation of BBB functions is mediated, at least in part, through continuous TGF-β production.

Acknowledgments

This work was supported, in part, by Grants-in-Aid for Scientific Research ((B)(2) 14370789) and ((C)(2) 15590475) from JSPS, Japan, by a Grant-in-Aid for Exploratory Research (16659138) from MEXT, Japan, and by funds (No. 031001) from the Central Research Institute of Fukuoka University and MEXT. HAITEKU (2000-2004). The authors thank Dr. Mária A. Deli, Institute of Biophysics, Biological Research Centre of the Hungarian Academy of Sciences for important comments on the preparation of the primary culture of pericytes.

References

[1] A. Antonelli-Orlidge, K.B. Saunders, S.R. Smith, P.A. D'Amore, An activated form of transforming growth factor β is produced by cocultures of endothelial cells and pericytes, Proc. Natl. Acad. Sci. U. S. A. 88 (1989) 4544–4548.

[2] R. Balabanov, P. Dore-Duffy, Role of the CNS microvascular pericyte in the blood–brain barrier, J. Neurosci. Res. 53 (1998) 637–644.

[3] V. Berezowski, C. Landry, M.-P. Dehouck, R. Cecchelli, L. Fenart, Contribution of glial cells and pericytes to the mRNA profiles of P-glycoprotein and multidrug resistance-associated proteins in an in vitro model of the blood–brain barrier, Brain Res. 1018 (2004) 1–9.
[4] M.M. Bradford, A rapid and sensitive method for the quantitation of microgram quantities of protein utilizing the principle of protein-dye binding, Anal. Biochem. 72 (1976) 248–254.
[5] M.-P. Dehouck, P. Jolliet-Riant, F. Brée, J.-C. Fruchart, R. Cecchelli, J.P. Tillement, Drug transfer across the blood–brain barrier: correlation between in vitro and in vivo models, J. Neurochem. 58 (1992) 1790–1797.
[6] R. Derynck, Y.E. Zhang, Smad-dependent and Smad-independent pathways in TGF-β family signaling, Nature 425 (2003) 577–584.
[7] S. Dohgu, Y. Kataoka, H. Ikesue, M. Naito, T. Tsuruo, R. Oishi, Y. Sawada, Involvement of glial cells in cyclosporine-increased permeability of brain endothelial cells, Cell. Mol. Neurobiol. 20 (2000) 781–786.
[8] S. Dohgu, A. Yamauchi, F. Takata, M. Naito, T. Tsuruo, S. Higuchi, Y. Sawada, Y. Kataoka, Transforming growth factor-β1 upregulates the tight junction and P-glycoprotein of brain microvascular endothelial cells, Cell. Mol. Neurobiol. 24 (2004) 491–497.
[9] D.B. Fee, D.L. Sewell, K. Andresen, T.J. Jacques, S. Piaskowski, B.A. Barger, M.N. Hart, Z. Fabry, Traumatic brain injury increases TGFβRII expression on endothelial cells, Brain Res. 1012 (2004) 52–59.
[10] G.A. Finlay, V.J. Thannickal, B.L. Fanburg, K.E. Paulson, Transforming growth factor-β1-induced activation of the ERK pathway/activator protein-1 in human lung fibroblasts requires the autocrine induction of basic fibroblast growth factor, J. Biol. Chem. 275 (2000) 27650–27656.
[11] K.C. Flanders, R.F. Ren, C.P. Lippa, Transforming growth factor-βs in neurodegenerative disease, Prog. Neurobiol. 54 (1998) 71–85.
[12] M. Fontaine, W.F. Elmquist, D.W. Miller, Use of rhodamine 123 to examine the functional activity of P-glycoprotein in primary cultured brain microvessel endothelial cell monolayers, Life Sci. 59 (1996) 1521–1531.
[13] K. Hayashi, S. Nakao, R. Nakaoke, S. Nakagawa, N. Kitagawa, M. Niwa, Effects of hypoxia on endothelial/pericytic co-culture model of the blood–brain barrier, Regul. Pept. 123 (2004) 77–83.
[14] K.K. Hirashi, P.A. D'Amore, Pericyte in the microvasculature, Cardiovasc. Res. 32 (1997) 687–698.
[15] S. Hori, S. Ohtsuki, K. Hosoya, E. Nakashima, T. Terasaki, A pericyte-derived angiopoietin-1 multimeric complex induces occludin gene expression in brain capillary endothelial cells through Tie-2 activation in vitro, J. Neurochem. 89 (2004) 503–513.
[16] J.D. Huber, R.D. Egleton, T.P. Davis, Molecular physiology and pathophysiology of tight junctions in the blood–brain barrier, Trends Neurosci. 24 (2001) 719–725.
[17] Y. Kim, R.Y. Imdad, A.H. Stephanson, R.S. Sprague, A.J. Lonigro, Vascular endothelial growth factor mRNA in pericytes is upregulated by phorbol myristate acetate, Hypertension 31 (1998) 511–515.
[18] S.W. Lee, W.J. Kim, Y.K. Choi, H.S. Song, H.S. Son, M.J. Son, I.H. Gelman, Y.J. Kim, K.W. Kim, SSeCKS regulates angiogenesis and tight junction formation in blood–brain barrier, Nat. Med. 9 (2003) 900–906.
[19] B.H. Liwnicz, J.L. Leach, H.-S. Yeh, M. Privitera, Pericyte degeneration and thickening of basement membranes of cerebral microvessels in complex parcial seizures: electron microscopic study of surgically removed tissue, Neurosurgery 26 (1997) 409–420.
[20] J. Massagué, TGF-β signal transduction, Annu. Rev. Biochem. 67 (1998) 753–791.
[21] A. Orlidge, P.A. D'Amore, Inhibition of capillary endothelial cell growth by pericytes and smooth muscle cells, J. Cell Biol. 105 (1987) 1455–1462.
[22] M. Ramsauer, D. Krause, R. Dermietzel, Angiogenesis of the blood–brain barrier in vitro and the function of cerebral pericytes, FASEB J. 16 (2002) 1274–1276.
[23] L.L. Rubin, J.M. Staddon, The cell biology of the blood–brain barrier, Annu. Rev. Neurosci. 22 (1999) 11–28.
[24] H.K. Rucker, H.J. Wynder, W.E. Thomas, Cellular mechanisms of CNS pericytes, Brain Res. Bull. 51 (2000) 363–369.
[25] Y. Sato, D.B. Rifkin, Inhibition of endothelial cell movement by pericytes and smooth muscle cells: activation of a latent transforming growth factor-β1-like molecular by plasmin during co-culture, J. Cell Biol. 109 (1989) 309–315.
[26] K. Sobue, N. Yamamoto, K. Yoneda, M.E. Hodgson, K. Yamashiro, N. Tsuruoka, T. Tsuda, H. Katsuya, Y. Miura, K. Asai, T. Kato, Induction of blood–brain barrier properties in immortalized bovine brain endothelial cells by astrocytic factors, Neurosci. Res. 35 (1999) 155–164.
[27] C.A. Szabó, M.A. Deli, T.K.D. Ngo, F. Joó, Production of pure primary rat cerebral endothelial cell culture: a comparison of different methods, Neurobiology 5 (1997) 1–16.
[28] T. Tatsuta, M. Naito, T. Oh-hara, I. Sugawara, T. Tsuruo, Functional involvement of P-glycoprotein in blood–brain barrier, J. Biol. Chem. 267 (1992) 20383–20391.
[29] T. Tatsuta, M. Naito, K. Mikami, T. Tsuruo, Enhanced expression by the brain matrix of P-glycoprotein in brain capillary endothelial cells, Cell Growth Differ. 5 (1994) 1145–1152.
[30] M.M. Verbeek, R.M. de Waal, J.J. Schipper, W.E. Van Nostrand, Rapid degeneration of cultured human brain pericytes by amyloid beta protein, J. Neurochem. 68 (1997) 1135–1141.
[31] W. Wang, M.J. Merrill, R.T. Borchardt, Vascular endothelial growth factor affects permeability of brain microvessel endothelial cells in vitro, Am. J. Physiol. 271 (1996) C1973–C1980.

Cellular and Molecular Neurobiology, Vol. 24, No. 6, October 2004 (© 2004)

Toxicity of Quinacrine Can Be Reduced By Co-Administration of P-Glycoprotein Inhibitor in Sporadic Creutzfeldt-Jakob Disease

Katsuya Satoh,[1] Susumu Shirabe,[1,5] Katsumi Eguchi,[1] Atsushi Yamauchi,[2] Yasufumi Kataoka,[2] Masami Niwa,[3] Noriyuki Nishida,[4] and Shigeru Katamine[4]

Received March 22, 2004; accepted April 12, 2004

SUMMARY

1. Recent publication has suggested that quinacrine may be a candidate for treatment of Creutzfeldt-Jakob disease (CJD). But serious toxicity of quinacrine to liver and hematological system has been reported.

2. We disclosed the permeability of quinacrine can be enhanced by presence of p-glycoprotein inhibitor at blood–brain barrier in vitro. Therefore, we tried the protocol of combination of quinacrine and p-glycoprotein inhibitor, verapamil for patients with CJD.

3. When compared clinical effects by quinacrine and the combination therapy, improvement of clinical findings was observed at the same level without any adverse effects. Low-dose quinacrine with verapamil can be used as safe treatment of CJD.

KEY WORDS: quinacrine; sporadic Creutzfeldt-Jakob disease; p-glycoprotein inhibitor.

INTRODUCTION

Although there are number of promising agents to control prion protein in vitro or in vivo, no sufficiently safe agent has yet been discovered for patients with Creutzfeldt-Jakob disease (CJD) (Doh-ura *et al.*, 2000).

Quinacrine, originally used as an anti-malaria agent, was reported as a possible agent useful for treatment of CJD (Korth *et al.*, 2001). Recent report found that quinacine might present serious toxicity to the liver and hematological system (Scoazec *et al.*, 2003).

[1] The First Department of Internal Medicine, Nagasaki University Graduate School of Biomedical Science, 1-7-1 Sakamoto, Nagasaki 852-8501, Japan.
[2] Department of Pharmaceutical Care and Health Sciences, Faculty of Pharmaceutical Sciences, Fukuoka University, 8-19-1 Nanakuma, Jo-nan ku, Fukuoka 812-8582, Japan.
[3] Department of Pharmacology, Nagasaki University Graduate School of Biomedical Science, 1-12-4 Sakamoto, Nagasaki 852-8501, Japan.
[4] Department of Molecular Microbiology and Immunology, Nagasaki University Graduate School of Biomedical Science, 1-12-4 Sakamoto, Nagasaki 852-8501, Japan.
[5] To whom correspondence should be addressed at Department of Internal Medicine, Nagasaki University Graduate School of Biomedical Science, 1-7-1 Sakamoto, Nagasaki 852-8501, Japan; e-mail: shirabe@net.nagasaki-u.ac.jp.

0272-4340/04/1200-0873/0

Quinacrine inhibited the accumulation of PrP^{Sc} in cultured infected cells, but did not have an apparent effect on PrP^{C} biosynthesis or turnover.

To develop some method of suppression of the adverse effects of quinacrine, we investigated the mechanism of quinacrine transport across the blood–brain barrier (BBB), and found that the permeability of quinacrine could be enhanced at the BBB by the presence of a p-glycoprotein inhibitor such as verapamil or cyclosporine (Dohgu *et al.*, 2003).

Therefore, we administrated a therapy regimen of combination of 200 mg/day of quinacrine and 120 mg/day of oral verapamil and compared it to one of 300–600 mg/day of quinacrine only.

We administrated quinacrine without verapamil for one patient, 64-year-old female who developed dementia and gait disturbance within two months. She was given 300 mg/day for the first two weeks, then the quantity was increased to 600 mg/day without p-glycoprotein inhibitor. Frequency of myoclonus, gaze, and smile were markedly improved. We stopped quinacrine administration due to liver dysfunction after four weeks. Two other sporadic CJD cases were treated by combination of quinacrine (200 mg/day) and verapamil (120 mg/day). The first case treated with combination therapy was a 71-year-old male, who had developed unstable gait, disorientation, and myoclonus. After two weeks administration of quinacrine and verapamil, frequency of myoclonus was dramatically decreased. Before starting medication, his eyes had rolled aimlessly. He began to gaze at his family and his doctor after the combination of quinacrine and verapamil. However, his symptoms returned to the non-medicated state after eight weeks, although he has been receiving medication.

The second case treated with combination therapy was a 65-year-old male. He was bedridden as a result of cerebellar ataxia and progressive dementia. Action myoclonus was observed. We started combination treatment of quinacrine and verapamil on him. After two weeks, his eye movement and myoclonus had improved markedly though the improvement was temporal. These three patients were diagnosed as possible CJD by based on clinical criteria of World Health Organization, diffusion-weighted MRI, and 14-3-3 protein in cerebrospinal fluid (CSF).

To determine whether quinacrine could be sufficiently transported to the brain, we measured the concentration of quinacrine in CSF at 4 weeks after administration of case in 2 and case 3 (Table I). Concentrations of quinacrine in CSF were measured by high-performance liquid chromatography method as described previously (Björkman and Elisson, 1987). The concentration of quinacrine in CSF, supposed to

Table I. Effects and Adverse Effects of Quinacrine in Patients with CJD

						Clinical effects	
Case	Co-administration	Concentration of quinacrine in CSF	AST level[a]	Hematological dysfunction	Skin color change	Frequency of myoclonus	Improvement of gaze and smile
1	None	ND	158	—	+	Decreased	+
2	Verapamil	392 nM	24	—	+	Decreased	+
3	Verapamil	226 nM	53	—	+	Decreased	+

Note. Plus symbol shows that each patient has the indicated findings.
[a]ALT; peak data under quinacrine administration.

be approximately equal to the concentration of quinacrine in experimental treatment in vitro approx. 200–400 nM (Korth *et al.*, 2001).

When the clinical effects on the first patient were compared with the other two patients (combination of 200 mg/day of quinacrine and 120 mg/day of verapamil), improvement of the clinical findings in patients receiving a combination of low dose quinacrine and verapamil was observed to be approximately equal to the level improvement seen in the patient receiving quinacrine only. In two patients treated with the combination of low-dose quinacrine and verapamil, no liver dysfunction and hematological toxicity was observed. Although French National Surveillance Network of Prion Diseases recommended to use quinacrine 1000 mg the first day, then 300 mg each day, we conclude that low-dose quinacrine can be used as a safe and effective treatment of CJD when given in combination with a p-glycoprotein inhibitor such as verapamil.

REFERENCES

Doh-ura, K., Mekada, E., Ogomori, K., and Iwaki, T. (2000). Enhanced CD9 expression in the mouse and human brains infected with transmissible spongiform encephalopathies. *J. Neuropathol. Exp. Neurol.* 59(9):774–785.

Korth, C., May, B. C., Cohen, F. E., and Prusiner, S. B. (2001). Acridine and phenothiazine derivatives as pharmacotherapeutics for prion disease. *Proc. Natl. Acad. Sci.* 98(17):9836–9841.

Scoazec, J. Y., Krolak-Salmon, P., Casez, O., Besson, G., Thobois, S., Kopp, N., *et al.* (2003). Quinacrine-induced cytolytic hepatitis in sporadic Creutzfeldt-Jakob disease. *Ann. Neurol.* 53(4):545–547.

Dohgu, S., Yamauchi, A., Takata, F., Sawada, Y., Higuchi, S., Naito, M., Tsuruo, T., Shirabe, S., Niwa, M., Katamine, S., and Kataoka, Y. (2003). Uptake and Efflux of Quinacrine, a Candidate for the Treatment of Prion Diseases at the Blood-Brain Barrier. *Cell Mol. Neurobiol.* (in press).

Björkman, S., and Elisson, L. O. (1987). Determination of quinacrine (mepacrine) in plasma by high-performance liquid chromatography with fluorimetric detection. *J Chromatograph* 420:341–348.

Available online at www.sciencedirect.com

SCIENCE DIRECT®

European Journal of Pharmacology 505 (2004) 51–59

ejp

www.elsevier.com/locate/ejphar

Nitric oxide mediates cyclosporine-induced impairment of the blood–brain barrier in cocultures of mouse brain endothelial cells and rat astrocytes

Shinya Dohgu[a], Atsushi Yamauchi[a], Shinsuke Nakagawa[b], Fuyuko Takata[a], Mamiko Kai[a], Takashi Egawa[a], Mikihiko Naito[c], Takashi Tsuruo[c], Yasufumi Sawada[d], Masami Niwa[b], Yasufumi Kataoka[a,*]

[a]*Department of Pharmaceutical Care and Health Sciences, Faculty of Pharmaceutical Sciences, Fukuoka University, 8-19-1 Nanakuma, Jonan-ku, Fukuoka 814-0180, Japan*

[b]*Department of Pharmacology 1, Nagasaki University Graduate School of Biomedical Sciences, 1-12-4 Sakamoto, Nagasaki 852-8523, Japan*

[c]*Institute of Molecular and Cellular Biosciences, University of Tokyo, Bunkyo-ku, Tokyo, 113-0032, Japan*

[d]*Department of Medico-Pharmaceutical Sciences, Graduate School of Pharmaceutical Sciences, Kyushu University, 3-1-1 Maidashi, Higashi-ku, Fukuoka 812-8582, Japan*

Received 8 October 2004
Available online 30 October 2004

Abstract

The present study was designed to clarify the involvement of nitric oxide (NO) signaling in the adverse effect of cyclosporine on the blood–brain barrier. Cyclosporine increased the permeability of sodium-fluorescein and the cellular accumulation of rhodamine 123, a substrate of P-glycoprotein, in mouse brain endothelial (MBEC4) cells. This effect was markedly enhanced two- to threefold when MBEC4 cells were cocultured with rat astrocytes or C6 glioma cells. Direct and continuous electrochemical measurement of NO demonstrated that cyclosporine dose-dependently increased histamine- and phenylephrine-evoked NO production in MBEC4 cells and astrocytes, respectively. A NO synthase inhibitor (N^G-monomethyl-L-arginine) blocked slightly and markedly cyclosporine-induced impairment of the endothelial barrier in the monolayer and coculture system, respectively. These findings suggest that cyclosporine impairs the brain endothelial barrier function by accelerating NO production in the brain endothelial and astroglial cells. This event may be interpreted as triggering the occurrence of cyclosporine neurotoxicity.

Keywords: Cyclosporine; Neurotoxicity; NO (nitric oxide); Blood–brain barrier; Permeability; P-glycoprotein

1. Introduction

Cyclosporine, a cyclic 11-amino acid peptide, is widely used as a potent immunosuppressant to prevent allograft rejection in solid organ transplantation and in fatal graft-vs.-host disease after bone marrow transplantation, and to treat various autoimmune diseases including rheumatoid arthritis (Kahan, 1989). Despite its high efficacy, cyclosporine has adverse effects including renal dysfunction, cardiovascular disorders, gastrointestinal disorders and neurological complications. These events occur with a relatively high frequency (20–40%) in organ-transplanted patients (Gijtenbeek et al., 1999; Pirsch et al., 1997; U.S. Group, 1994).

The entry of cyclosporine into the brain is prevented by the tight junctions and P-glycoprotein, a multi-drug efflux pump, of the brain microvascular endothelial cells. But the adverse neurological effects of cyclosporine, including tremors, seizures and encephalopathy, strongly suggest the possibility of cyclosporine transport across the blood–brain

* Corresponding author. Tel./fax: +81 92 862 2696.
E-mail address: ykataoka@cis.fukuoka-u.ac.jp (Y. Kataoka).

0014-2999/$ - see front matter © 2004 Elsevier B.V. All rights reserved.
doi:10.1016/j.ejphar.2004.10.027

barrier. We previously reported that cyclosporine produced convulsions by inhibiting γ-aminobutyric acid (GABA)-ergic neural activity and binding properties of the $GABA_A$ receptor (Shuto et al., 1999). The inhibition of GABAergic neurotransmission by cyclosporine may lead to an activation of serotonergic neural activity and consequently produce tremors (Shuto et al., 1998). These findings in vivo are considered to be due to a direct action of cyclosporine transported across the blood–brain barrier rather than an indirect effect through the periphery. In fact, we demonstrated that cyclosporine at a high concentration decreased the function and expression of P-glycoprotein in brain capillary endothelial cells (Kochi et al., 1999; 2000). The blood–brain barrier is primarily formed by brain capillary endothelial cells, which are closely sealed by tight junctions (Partridge, 1999). P-glycoprotein is abundantly expressed in the brain endothelial cells and limits the accumulation of many hydrophobic molecules and toxic substances in the brain (Schinkel, 1999). Recently, we demonstrated that nitric oxide (NO) increased the permeability and inhibited the P-glycoprotein efflux pump of brain capillary endothelial cells, suggesting that NO impairs the dynamic regulation of the blood–brain barrier function (Yamauchi et al., in press). Astrocytes and pericytes are cellular components of the blood–brain barrier. Astrocytes surround the cerebral capillaries and regulate blood–brain barrier function through cell-to-cell contact and secretion of soluble factors (Terasaki et al., 2003).

The present study was designed to clarify the involvement of NO signaling in the adverse effect of cyclosporine on the blood–brain barrier. We first evaluated the effect of cyclosporine on the permeability and the P-glycoprotein function of mouse brain endothelial (MBEC4) cells alone and cocultured with rat astrocytes or C6 glioma cells. Second, the effect of cyclosporine on the stimulation-evoked NO production was examined in MBEC4 cells and rat astrocytes using direct electrochemical NO monitoring.

2. Materials and methods

2.1. Materials

Cyclosporine was kindly supplied by Novartis Pharma (Bazel, Switzerland). Sodium fluorescein (Na-F, MW 376), rhodamine 123, phenylephrine hydrochloride, histamine, L-arginine and N^G-monomethyl-L-arginine (L-NMMA) were purchased from Sigma (St. Louis, MO, USA). Culture medium and subculture reagents were obtained from Invitrogen (Carlsbad, CA, USA). All remaining reagents of analytical grade were purchased from Wako (Osaka, Japan).

2.2. Animals

Wistar rats aged 3 days old were used in this study. All the procedures involving experimental animals adhered to the law (No. 105) and notification (No. 6) of the Japanese Government, and were approved by the Laboratory Animal Care and Use Committee of Fukuoka University.

2.3. Cell culture

MBEC4 cells, which were isolated from BALB/c mouse brain cortices and immortalized by SV40-transformation (Tatsuta et al., 1992), were cultured in Dulbecco's modified Eagle's medium (DMEM) supplemented with 10% fetal bovine serum, 100 units/ml penicillin and 100 μg/ml streptomycin. C6 glioma cells (JCRB9096, Health Science Research Resources Bank, Osaka, Japan) were cultured in DMEM supplemented with 10% fetal calf serum, and 50 μg/ml gentamicin. Newborn rat astrocytes were isolated according to the method of McCarthy and de Vellis (1980) and Sastradipura et al. (1998) with a slight modification. Briefly, the cerebral cortex from 3-day-old rats was minced and treated with papain (90 units/ml; Worthington, Lakewood, NJ) and DNase I (2000 units/ml; Sigma) at 37 °C for 15 min. The mechanically dissociated cells were seeded into plastic flasks in DMEM supplemented with 10% fetal bovine serum, 100 units/ml penicillin and 100 μg/ml streptomycin. After 10–14 days in culture, floating cells and weakly attached cells on the mixed primary cultured cell layer were removed by vigorous shaking of the flask. Then, astrocytes on the bottom of the culture flask were trypsinized and seeded into new culture flasks. The primary cultured astrocytes were maintained in DMEM. They were grown in a humidified atmosphere of 5% CO_2/95% air at 37 °C.

The preparation of the in vitro blood–brain barrier models has been described previously (Dohgu et al., 2000). In brief, C6 cells or rat astrocytes (40,000 cells/cm^2) were first cultured on the outside of the collagen-coated polycarbonate membrane (3.0 μm pore size) of the Transwell™ insert (12-well type, Costar, MA, USA) directed upside down in the well. Two days later, MBEC4 cells (42,000 cells/cm^2) were seeded on the inside of the insert placed in the well of the 12-well culture plate (Costar) (C6 coculture and rat astrocyte coculture). The monolayer system was also made with MBEC4 cells alone (MBEC4 monolayer).

2.4. Treatment with cyclosporine and nitric oxide (NO) synthase inhibitor

Cyclosporine was first dissolved in ethanol and diluted with serum-free culture medium (0.1% as the final ethanol concentration). MBEC4 cells were cultured for 3 days, and these inserts were washed three times with serum-free medium. Then cells were exposed to 1–5 μM cyclosporine injected into the inside of the insert (luminal side) for 12 h. When the effect of NO synthase (NOS) inhibitor was examined, L-NMMA (1 mM) was loaded both inside and outside of the insert (luminal and abluminal side). In

parallel, cells were treated with serum-free medium containing the corresponding amount of ethanol as the vehicle.

2.5. Paracellular transport of Na-F

To initiate the transport experiments, the medium was removed and MBEC4 cells were washed three times with Krebs–Ringer buffer (118 mM NaCl, 4.7 mM KCl, 1.3 mM $CaCl_2$, 1.2 mM $MgCl_2$, 1.0 mM NaH_2PO_4, 25 mM $NaHCO_3$, and 11 mM D-glucose, pH 7.4). Krebs–Ringer buffer (1.5 ml) was added to the outside of the insert (abluminal side). Krebs–Ringer buffer (0.5 ml) containing 100 μg/ml of Na-F was loaded on the luminal side of the insert. Samples (0.5 ml) were removed from the abluminal chamber at 10, 20, 30 and 60 min and immediately replaced with fresh Krebs–Ringer buffer. Aliquots (5 μl) of the abluminal medium were mixed with 200 μl of Krebs–Ringer buffer and then the concentration of Na-F was determined using a fluorescence multiwell plate reader (Ex(λ) 485 nm; Em(λ) 530 nm) (CytoFluor Series 4000, PerSeptive Biosystems, Framingham, MA, USA). The permeability coefficient and clearance were calculated according to the method described by Dehouck et al. (1992). Clearance was expressed as microliters (μl) of tracer diffusing from the luminal to abluminal chamber and was calculated from the initial concentration of tracer in the luminal chamber and final concentration in the abluminal chamber: Clearance (μl)=$[C]_A \times V_A/[C]_L$ where $[C]_L$ is the initial luminal tracer concentration, $[C]_A$ is the abluminal tracer concentration and V_A is the volume of the abluminal chamber. During a 60-min period of the experiment, the clearance volume increased linearly with time. The average volume cleared was plotted vs. time, and the slope was estimated by linear regression analysis. The slope of clearance curves for the MBEC4 monolayer or coculture systems was denoted by PS_{app}, where PS is the permeability-surface area product (in μl/min). The slope of the clearance curve with a control membrane was denoted by $PS_{membrane}$. In the coculture system, the control membrane is the C6 cell- or rat astrocyte-layered membrane. The real PS value for the MBEC4 monolayer and the coculture system (PS_{trans}) was calculated from $1/PS_{app}=1/PS_{membrane}+1/PS_{trans}$. The PS_{trans} values were divided by the surface area of the Transwell inserts to generate the permeability coefficient (P_{trans}, in cm/min).

2.6. Functional activity of P-glycoprotein

The functional activity of P-glycoprotein was determined by measuring the cellular accumulation of rhodamine 123 (Sigma) according to the method of Fontaine et al. (1996). MBEC4 cells were washed three times with assay buffer (143 mM NaCl, 4.7 mM KCl, 1.3 mM $CaCl_2$, 1.2 mM $MgCl_2$, 1.0 mM NaH_2PO_4, 10 mM HEPES, and 11 mM D-glucose, pH 7.4). In both coculture systems, C6 cells and rat astrocytes on the outside of the membrane were removed with a cell scraper. MBEC4 cells were incubated with 0.5 ml of assay buffer containing 5 μM of rhodamine 123 for 60 min. Then, the solution was removed and the cells were washed three times with ice-cold phosphate-buffered saline and solubilized in 1 M NaOH (0.2 ml). The solution was neutralized with 1 M HCl (0.2 ml) and the rhodamine 123 content was determined using a fluorescence multiwell plate reader (Ex(λ) 485 nm; Em(λ) 530 nm, CytoFluor Series 4000). The cellular protein was measured by the method of Bradford (1976).

2.7. Electrochemical monitoring of NO

Direct and continuous electrochemical measurement of NO was performed with a three-electrode potentiostatic EMS-100 system (BIO-LOGIC, Grenoble, France) as previously described (Ikesue et al., 2000, Trevin et al., 1998). In brief, confluent MBEC4 cells or rat astrocytes in a 2.5 cm^2 dish (BD FALCON™, BD Biosciences, NJ, USA) were washed three times with Mg^{2+}-free Krebs–Ringer solution (143.0 mM NaCl, 4.7 mM KCl, 2.5 mM $CaCl_2$, 1.0 mM NaH_2PO_4 and 11.0 mM D-glucose, pH 7.4). The dish was placed on the stage of an inverted microscope (ECLIPSE TE300, Nikon, Tokyo, Japan) mounted with a NO monitoring system. The NO-biosensor (ASTEC, Fukuoka, Japan) was positioned about 10 μm above the cell surface. Ten minutes after treatment with L-arginine (1 mM), histamine or phenylephrine in a volume of 10 μl was added to the cells in 1 ml of Mg^{2+}-free Krebs–Ringer solution with a transient mixing step to give the final concentration indicated. The level of production of NO in MBEC4 cells or rat astrocytes was monitored for a 15-min period after the addition of histamine or phenylephrine. Cyclosporine was added 20 min before treatment with L-arginine.

2.8. Assessment of cell viability

The effect of cyclosporine on the viability of cells in the MBEC4 monolayer, C6 coculture and rat astrocyte coculture systems was assessed using a WST-8 assay (Cell Counting Kit-8, DOJINDO, Kumamoto, Japan). A highly water-soluble formazan dye (WST-8), reduced by mitochondrial dehydrogenase, was measured by determining the absorbance of each sample with a 450 nm test wavelength and a 700 nm reference wavelength using a microplate reader (Opsys MR, DYNEX technologies, Chantilly, VA, USA).

2.9. Measurement of NO Production using NO-specific dye

An accumulation of NO production during a 12 h period was assessed using a NO-specific fluorescent dye, 4,5-diaminofluorescein diacetate (DAF-2 DA, Sigma) (Nakatsubo et al., 1998). MBEC4 and C6 cells were seeded on wells of the 24-well culture plate. Cells were

incubated with DAF-2 DA at a final concentration of 10 μM for 1 h at 37 °C and then rinsed three times with serum-free medium. Cells containing DAF2 DA were exposed to cyclosporine (1–5 μM) for 12 h and they were washed three times with assay buffer (143 mM NaCl, 4.7 mM KCl, 1.3 mM $CaCl_2$, 1.2 mM $MgCl_2$, 1.0 mM NaH_2PO_4, 10 mM HEPES, and 11 mM D-glucose, pH 7.4). The fluorescence was measured using a fluorescence multiwell plate reader (Ex(λ) 485 nm; Em(λ) 530 nm, CytoFluor Series 4000). Then, cells were solubilized with 250 μl of 1 M NaOH. Aliquots of the cell solution were removed for protein assay according to the method of Bradford using a Bio-Rad protein assay kit (Bio-Rad Laboratories, Hercules, CA) (Bradford, 1976). Data for each experiment were normalized to the cellular protein.

2.10. Statistical analysis

The values are expressed as the means±S.E.M. Statistical analysis was performed using Student's *t*-test. One way and two way analyses of variance (ANOVAs) followed by Tukey–Kramer's tests were applied to multiple comparisons. The differences between means were considered to be significant when *P* values were less than 0.05.

3. Results

3.1. Permeability and P-glycoprotein function of MBEC4 cells in MBEC4 monolayer, C6 coculture and rat astrocyte coculture systems

After MBEC4 cells were cultured for 3 days, the basal permeability and P-glycoprotein efflux pump of MBEC4 cells were evaluated in three in vitro blood–brain barrier models (Fig. 1). The permeability coefficient of Na-F for MBEC4 cells was increased by 57.6% in the C6 coculture and reduced by 45.6% in the rat astrocyte coculture, when compared to that in the MBEC4 monolayer (Fig. 1A). The accumulation of rhodamine 123 in MBEC4 cells was significantly increased by 16.8% in the C6 coculture and significantly reduced by 17.9% in the rat astrocyte coculture relative to the MBEC4 monolayer (Fig. 1B).

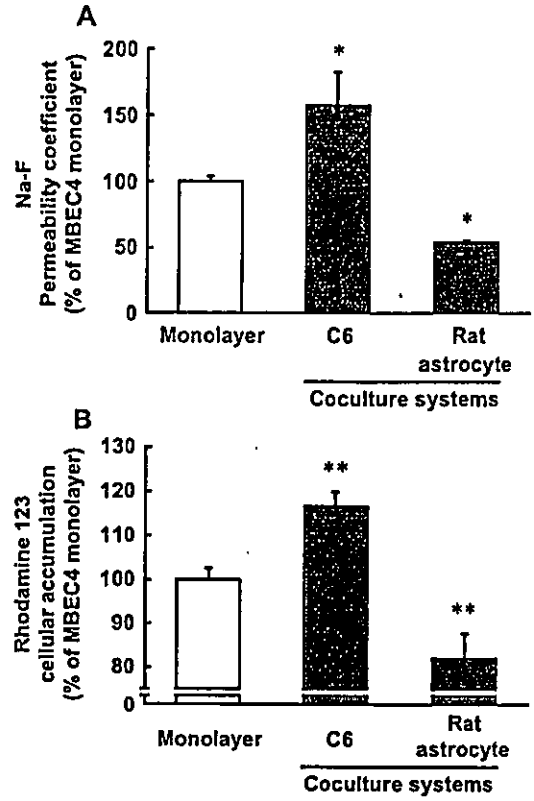

Fig. 1. Permeability and P-glycoprotein function of MBEC4 cells in MBEC4 monolayer, C6 coculture and rat astrocyte coculture systems. (A) MBEC4 permeability coefficients of Na-F. Results are expressed as % of the MBEC4 monolayer ($1.88\pm0.10\times10^{-4}$ cm/min). Values are the means± S.E.M. (n=3–7). *P<0.05, significant difference from MBEC4 monolayer. (B) Rhodamine 123 accumulation in MBEC4 cells. Results are expressed as % of the MBEC4 monolayer (2.19±0.16 nmol/mg protein). Values are the means±S.E.M. (n=4–17). **P<0.01, significant difference from MBEC4 monolayer.

3.2. Effect of cyclosporine on permeability and P-glycoprotein function of MBEC4 cells in MBEC4 monolayer, C6 coculture and rat astrocyte coculture systems

As shown in Figs. 2 and 3, the exposure to cyclosporine (1–5 μM) for 12 h dose-dependently increased the permeability of Na-F and the cellular accumulation of rhodamine 123 in the MBEC4 monolayer and C6 coculture. The Na-F permeability and the rhodamine 123 accumulation of MBEC4 cells in the rat astrocyte coculture were increased to 127.7±7.2% and 126.7±3.0% of vehicle by 5 μM cyclosporine. These adverse effects of cyclosporine in the presence of C6 cells and astrocytes were two- to threefold more potent than the effects in the MBEC4 monolayer.

The WST-8 assay showed that cyclosporine at the highest concentration tested (5 μM) had no effect on cell viability in any of the three culture systems (MBEC4 monolayer: 98.2±1.00, C6 coculture: 101.2±1.79, rat astrocyte coculture: 103.9±7.5% of the corresponding vehicle).

3.3. Effect of cyclosporine on stimulation-evoked NO production and spontaneous NO production in MBEC4 cells, rat astrocytes and C6 cells

Cyclosporine alone at concentrations less than 5 μM failed to stimulate NO production to a detectable level (Fig. 4). In the absence of cyclosporine, histamine (100 μM) and phenylephrine (1 μM) produced small amounts of NO in MBEC4 cells and rat astrocytes (9.27±0.69 and 0.32±0.036 μM), respectively (Fig. 4). Cyclosporine (1, 2 and 5 μM) dose-dependently increased histamine (100 μM)- and phenylephrine (1 μM)-evoked NO production in MBEC4 cells and astrocytes, respectively (Fig. 4). The increases induced by 5 μM cyclosporine reached

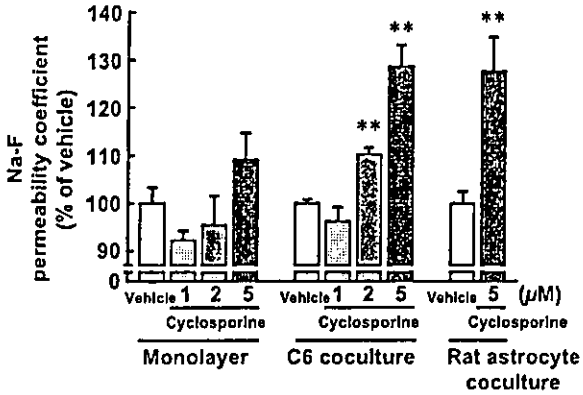

Fig. 2. Effect of cyclosporine on MBEC4 permeability of Na-F in MBEC4 monolayer, C6 coculture and rat astrocyte coculture systems. Transport experiments were performed after 12 h of exposure to cyclosporine. Results are expressed as % of each corresponding vehicle (monolayer; $2.35\pm0.24\times10^{-4}$ cm/min, C6 coculture; $2.34\pm0.25\times10^{-4}$ cm/min, rat astrocyte coculture; $1.16\pm0.03\times10^{-4}$ cm/min). Values are the means± S.E.M. (n=3–24). **P<0.01, significant difference from each corresponding vehicle.

174.1±7.7% and 198.2±15.0% of vehicle in MBEC4 cells and astrocytes, respectively.

When total amounts of NO production during a 12 h period was measured using a NO-specific fluorescent dye, an exposure of cyclosporine (5 μM) for 12 h significantly increased spontaneous (basal) NO production by 70 and 190% in MBEC4 and C6 cells, respectively (Fig. 5).

3.4. Effect of NO synthase inhibitor on cyclosporine-increased permeability of Na-F and accumulation of rhodamine 123 in MBEC4 monolayer and rat astrocyte coculture systems

L-NMMA (1 mM) (a NOS inhibitor) alone had no effect on the permeability of Na-F and the accumulation of rhodamine 123 in the MBEC4 monolayer and C6 coculture.

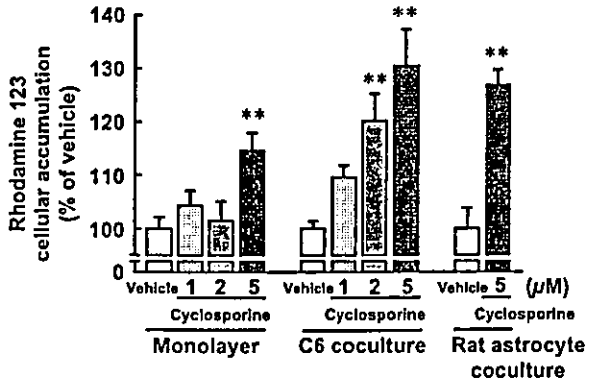

Fig. 3. Effect of cyclosporine on rhodamine 123 accumulation in MBEC4 cells of the MBEC4 monolayer, C6 coculture and rat astrocyte coculture systems. P-glycoprotein function was evaluated after 12 h of exposure to cyclosporine. Results are expressed as % of each corresponding vehicle (monolayer; 3.50±0.56 nmol/mg protein, C6 coculture; 3.79±0.47 nmol/mg protein, rat astrocyte coculture; 0.85±0.04 nmol/mg protein). Values are the means±S.E.M. (n=4–20). **P<0.01, significant difference from each corresponding vehicle.

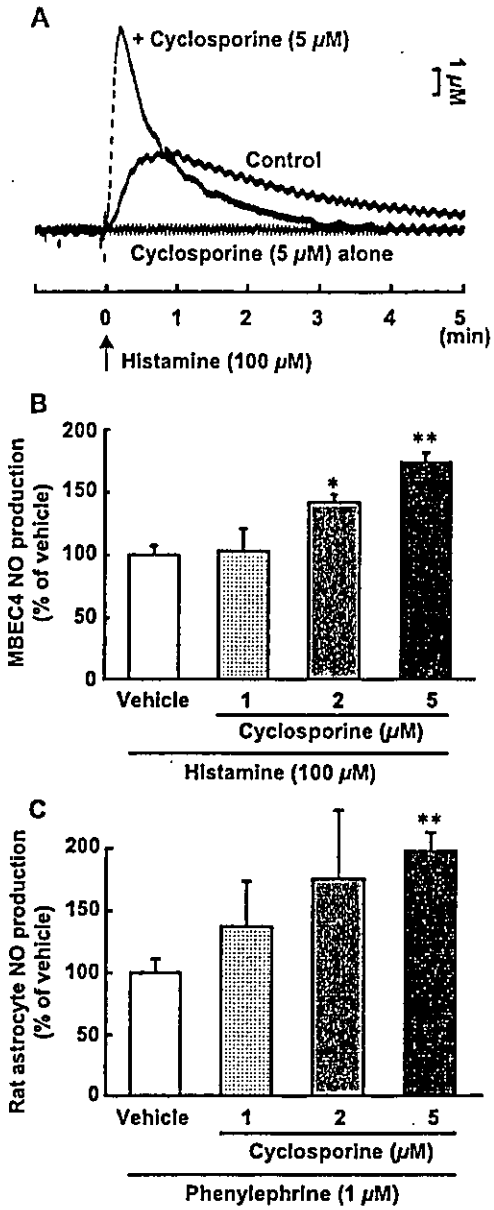

Fig. 4. Effect of cyclosporine on stimulations-evoked NO production. (A) Representative differential pulse amperogram obtained using NO biosensor shows NO production evoked by histamine (100 μM) in the absence (Control, middle trace) and presence of cyclosporine (5 μM) (+cyclosporine, top trace) in MBEC4 cells. The effect of cyclosporine (5 μM) alone on NO production was indicated in the bottom trace. (B) Concentration-dependent facilitatory effect of cyclosporine on histamine-evoked NO production in MBEC4 monolayer. Results are expressed as % of histamine (100 μM)-evoked NO production (vehicle; 9.27±0.69 μM). Values are the means± S.E.M. (n=3). *P<0.05 and **P<0.01, significant differences from vehicle. (C) Concentration-dependent facilitatory effect of cyclosporine on phenylephrine-evoked NO production in rat astrocyte coculture system. Results are expressed as % of phenylephrine (1 μM)-evoked NO production (vehicle; 0.32±0.036 μM). Values are the means±S.E.M. (n=4–7). *P<0.05 and **P<0.01, significant differences from vehicle.

Cyclosporine (5 μM)-increased permeability of Na-F and accumulation of rhodamine 123 in MBEC4 cells were significantly decreased to 114.3±5.9% and 112.6±3.7% of

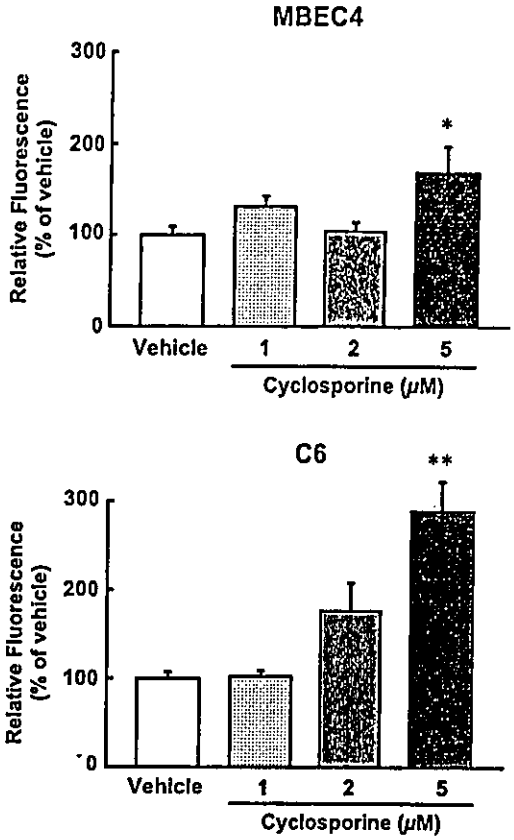

Fig. 5. Effect of cyclosporine on spontaneous NO production in MBEC4 and C6 cells. Cells were loaded with a NO-specific fluorescent dye (DAF-2 DA) and then treated with 1–5 μM cyclosporine for 12 h. The fluorescence intensity of DAF-2 DA was increased by NO produced by cells and this was normalized to the cellular protein. Relative fluorescence is expressed as the ratio (%) to the control value obtained in the absence of cyclosporine (vehicle). Values are the means±S.E.M. (n=8). *P<0.05, significant differences from vehicle.

vehicle, respectively, by 1 mM L-NMMA in the C6 coculture (Fig. 6). In contrast, L-NMMA (1 mM) produced a slight inhibition of the permeability of Na-F and the accumulation of rhodamine 123 induced by Cyclosporine (5 μM) in the MBEC4 monolayer (Fig. 6).

4. Discussion

We made three types of the in vitro blood–brain barrier models; MBEC4 monolayer, C6 coculture, and rat astrocyte coculture systems. MBEC4 cells alone show the highly specialized characteristics of brain microvascular endothelial cells including the integration of tight junctions and expression of P-glycoprotein (Tatsuta et al., 1992, 1994). Astrocytes, a cellular component of the blood–brain barrier, induce and maintain the functioning of the blood–brain barrier through cell-to-cell contact and the secretion of soluble factors (Rubin and Staddon, 1999). The barrier function in these models was evaluated based on the permeability of Na-F and the P-glycoprotein efflux pump of MBEC4 cells. Na-F was used as a marker of permeability through the paracellular route. The permeability and the accumulation of rhodamine 123 in MBEC4 cells were markedly decreased in the presence of rat astrocytes (Fig. 1). These findings suggest that astrocytes participate in tightening the intercellular junctions and facilitating P-glycoprotein function of brain endothelial cells. A positive role for astrocytes in the expression and maintenance of endothelial tight junctions has been documented (Dehouck et al., 1992; Gaillard et al., 2001; Isobe et al., 1996; Rauh et al., 1992; Hayashi et al., 1997), although there are few reports concerning astrocyte-enhanced P-glycoprotein function. The C6 cell line, which originated from rat glioma cells, is commonly used as an experimental model of astrocytes due to convenient handling (Zhang et al., 2004). The barrier function of MBEC4 cells was speculated to be

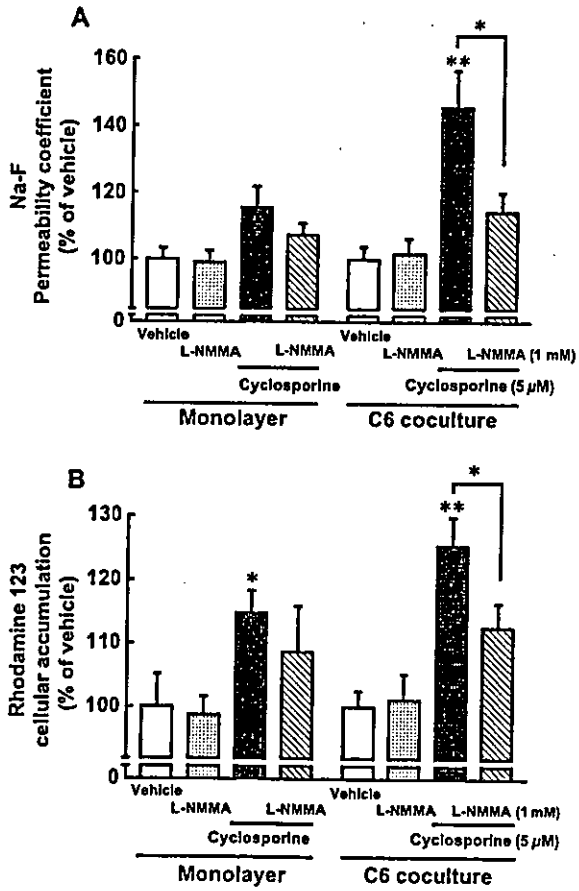

Fig. 6. Effect of NO synthase inhibitor (L-NMMA) on cyclosporine-increased MBEC4 permeability of Na-F (A), and rhodamine 123 accumulation in MBEC4 cells (B) in MBEC4 monolayer and C6 coculture system. (A) Results are expressed as % of each corresponding vehicle (monolayer; $1.73\pm0.10\times10^{-4}$ cm/min, C6 coculture; $2.95\pm0.55\times10^{-4}$ cm/min). Values are the means±S.E.M. (n=7–11). *P<0.05, **P<0.01, significant difference from each corresponding vehicle. (B) Results are expressed as % of each corresponding vehicle (monolayer; 14.2±3.94 nmol/mg protein, C6 coculture; 9.05±2.00 nmol/mg protein). Values are the means±S.E.M. (n=7–12). *P<0.05, **P<0.01, significant differences from each corresponding vehicle.

enhanced by the C6 cells similar the rat astrocyte coculture. However, the present findings indicated hyperpermeability of Na-F and reduced P-glycoprotein function in the C6 coculture. These results may be due to neoplastic changes in the glial characteristics. The precise mechanism by which C6 cells affect the barrier function of MBEC4 cells is now under investigation. There were no apparent differences in the endothelial cell response to cyclosporine between the C6 coculture and rat astrocyte coculture (Figs. 2 and 3). This confirms that the C6 coculture model is suitable for pharmacological research.

Cyclosporine-induced neurotoxicity including tremors, convulsions and encephalopathy occurred frequently in patients with high blood concentrations of cyclosporine, although these concentrations were within the therapeutic range (Gijtenbeek et al., 1999). The maximal blood concentrations of cyclosporine in patients with renal or liver transplantation are known to be in the range varying from 1 to 1.5 μM (Kahan et al., 1995; Keown and Niese, 1998; Grant et al., 1999). Therefore, the concentrations (1–5 μM) of cyclosporine used in the present study are less than three- to fivefold level of the maximal concentrations in patients. Cyclosporine (5 μM) significantly increased the permeability of Na-F and the accumulation of rhodamine 123 in the MBEC4 monolayer. These effects were potentiated markedly in the coculture with C6 cells or rat astrocytes (Figs. 2 and 3). Then, we substituted C6 cells for the primary culture of rat astrocytes to save the experimental animals, costs and labor in the subsequent pharmacological study. The presence of C6 cells increased by two- to threefold the facilitatory and inhibitory effects of cyclosporine (1–5 μM) on the paracellular permeability and P-glycoprotein activity of the MBEC4 monolayer, respectively. These effects were not due to the direct cytotoxicity of cyclosporine. These findings indicated that cyclosporine reduces the barrier function of brain endothelial cells to penetrate into the brain, leading to further aggravation of the blood–brain barrier function by interacting with astrocytes.

A 12-h exposure of cyclosporine (5 μM) in the same schedule as the blood–brain barrier function test significantly increased the accumulation of spontaneous NO production during a 12-h period, when measured using a NO-specific fluorescent dye (Fig. 5). A direct electrochemical NO monitoring failed to detect cyclosporine-increased basal NO production (Fig. 4). This monitoring method is capable of detecting a rapid NO production in response to the stimulation as a sharp current–time curve, even if amounts of NO production are small. However, NO biosensor is relatively difficult to detect a slow NO production with a low peak and a long-lasting plateau phase, even if total amounts during a long period is large. Cyclosporine dose-dependently enhanced histamine- and phenylephrine-evoked NO production in MBEC4 cells and rat astrocytes, respectively (Fig. 4). Cyclosporine exerts pharmacological effects by binding to cyclophilin (peptidyl-propyl isomerase), a highly basic and abundant cytosolic protein (Marks, 1996). This cyclosporine/cyclophilin complex inhibits calcineurin, a serine–threonine phosphatase 2B, thereby blocking its phosphatase activity (Marks, 1996; Yakel, 1997). Calcineurin regulates the activity of ion channels and neurotransmitter release. Calcineurin anchored to the inositol 1,4,5-triphosphate (IP_3) receptor via FKBP12, a FK506-binding protein, regulates the phosphorylation status of the receptor, resulting in a dynamic Ca^{2+}-sensitive regulation of IP_3-mediated Ca^{2+} flux (Cameron et al., 1997). In contrast with FKBP12, cyclophilin does not bind to the IP_3 receptor (Cameron et al., 1995). However, when rat cerebellar microsomes were treated with cyclosporine and cyclophilin, protein kinase C-induced IP_3 receptor phosphorylation and IP_3-stimulated Ca^{2+} flux were markedly increased (Cameron et al., 1995). This suggests that cyclosporine inhibits the dephosphorylation of the IP_3 receptor to maintain a leaky IP_3 receptor channel that was phosphorylated by serine–threonine protein kinases such as protein kinase C. Although the IP_3 receptor becomes leaky, cyclosporine alone appears incapable of elevating $[Ca^{2+}]_{IN}$ over the threshold for activation of the constitutive NO synthase. This may explain the present findings that cyclosporine alone failed to raise NO production above the detection limit of the NO biosensor, while the histamine and phenylephrine-evoked NO production in MBEC4 and C6 cells, respectively, was markedly facilitated by cyclosporine. Histamine and phenylephrine activate phospholipase C through the H_1 receptor and α_1-adrenoceptor, respectively, to generate IP_3 (Lum and Malik, 1994; Daum et al., 1983) and stimulate the leaky Ca^{2+} channel (phosphorylation status of IP_3 receptor) maintained by cyclosporine. These events probably lead to the markedly higher level of $[Ca^{2+}]_{IN}$ than that induced by histamine and phenylephrine in MBEC4 cells and rat astrocytes, respectively. We previously reported that cyclosporine also enhanced α_1-adrenoceptor-mediated NO production in C6 cells (Ikesue et al., 2000). In the brain, various biological substances including noradrenaline, glutamate, histamine and endothelin stimulate G protein-coupled receptors that have a common intracellular signaling pathway (IP_3/diacylglycerol) in astrocytes (Verkhratsky and Kettenmann, 1996). This endogenous stimulator-evoked NO production is highly likely to be augmented by cyclosporine via a mechanism similar to that proposed here. In fact, our in vivo microdialysis experiment showed that an intraperitoneal injection of cyclosporine significantly increased NO production in the rat dorsal hippocampus (Fujisaki et al., 2002).

The present study demonstrated that cyclosporine impaired the barrier function of brain endothelial cells and this effect was remarkably potentiated by co-culturing MBEC4 cells with C6 cells or rat astrocytes. A NO synthase inhibitor, L-NMMA at a concentration of 1 mM showed no effect on the Na-F permeability and the rhodamine 123 accumulation of MBEC4 cells in both culture systems (Fig. 6), suggesting that L-NMMA (1 mM)

has not nonspecific effect on the basal blood–brain barrier functions of MBEC4 cells. L-NMMA (1 mM) significantly blocked the cyclosporine-induced increase in the permeability of Na-F and accumulation of rhodamine 123 in the C6 coculture. This protective effect was moderate in the MBEC4 monolayer (Fig. 6). These findings suggest that cyclosporine-enhanced NO production in astrocytes largely contributes to an impairment of the blood–brain barrier. This notion is supported by our previous findings that NO lowered the function of tight junctions and P-glycoprotein at the blood–brain barrier (Yamauchi et al., in press). The mechanisms by which NO donors increased vascular endothelial permeability involved an increase in the level of cGMP (Gimeno et al., 1998) or the formation of peroxynitrite (Menconi et al., 1998). These substances conceivably influence intrinsic tight junction proteins and the associated actin cytoskeleton through a direct or second signaling pathway (Burgstahler and Nathanson, 1995; Liu and Sundqvist, 1997). It is, therefore, likely that cyclosporine passes through the slightly impaired barrier of brain endothelial cells and then acts on astrocytes to enhance NO production, leading to further aggravation of the blood–brain barrier impairment.

In conclusion, cyclosporine accelerated stimulation-evoked NO production in brain endothelial and astroglial cells. This enhanced production of NO that interacts with each cellular component of the blood–brain barrier is involved in the sequential process of blood–brain barrier functional impairment induced by cyclosporine.

Acknowledgements

This work was supported, in part, by Grants-in-Aid for Scientific Research ((B)(2) 14370789) and ((C)(2) 15590475) from JSPS, Japan, by a Grant-in-Aid for Exploratory Research (16659138) from MEXT, Japan and by funds (No.: 031001) from the Central Research Institute of Fukuoka University.

References

Bradford, M.M., 1976. A rapid and sensitive method for the quantitation of microgram quantities of protein utilizing the principle of protein-dye binding. Anal. Biochem. 72, 248–254.

Burgstahlar, A.D., Nathanson, M.H., 1995. NO modulates the apicolateral cytoskeleton of isolated hepatocytes by a PKC-dependent, cGMP-independent mechanism. Am. J. Physiol. 276, G789–G799.

Cameron, A.M., Steiner, J.P., Roskams, A.J., Ali, S.M., Ronnett, G.V., Snyder, S.H., 1995. Calcineurin associated with the inositol 1,4,5-trisphosphate receptor-FKBP12 complex modulates Ca^{2+} flux. Cell 83, 463–472.

Cameron, A.M., Nucifora, F.C., Fung, E.T., Livingston, D.J., Aldape, R.A., Ross, C.A., Snyder, S.H., 1997. FKBP12 binds the inositol 1,4,5-trisphosphate receptor at leucine-proline (1400–1401) and anchors calcineurin to this FK506-like domain. J. Biol. Chem. 272, 27582–27588.

Daum, P.R., Downes, C.P., Young, J.M., 1983. Histamine-induced inositol phospholipids breakdown mirrors H_1-receptor density in brain. Eur. J. Pharmacol. 87, 497–498.

Dehouck, M.-P., Jolliet-Riant, P., Brée, F., Fruchart, J.-C., Cecchelli, R., Tillement, J.-P., 1992. Drug transfer across the blood–brain barrier: correlation between in vitro and in vivo models. J. Neurochem. 58, 1790–1797.

Dohgu, S., Kataoka, Y., Ikesue, H., Naito, M., Tsuruo, T., Oishi, R., Sawada, Y., 2000. Involvement of glial cells in cyclosporine-increased permeability of brain endothelial cells. Cell. Mol. Neurobiol. 20, 781–786.

Fontaine, M., Elmquist, W.F., Miller, D.W., 1996. Use of rhodamine 123 to examine the functional activity of P-glycoprotein in primary cultured brain microvessel endothelial cell monolayers. Life Sci. 59, 1521–1531.

Fujisaki, Y., Yamauchi, A., Dohgu, S., Sunada, K., Yamaguchi, C., Oishi, R., Kataoka, Y., 2002. Cyclosporine A-increased nitric oxide production in the rat dorsal hippocampus mediates convulsions. Life Sci. 72, 549–556.

Gaillard, P.J., Voorwinden, L.H., Nielsen, J.L., Ivanov, A., Atsumi, R., Engman, H., Ringbom, C., de Boer, A.G., Breimer, D.D., 2001. Establishment and functional characterization of an in vitro model of the blood–brain barrier, comprising a co-culture of brain capillary endothelial cells and astrocyte. Eur. J. Pharm. Sci. 12, 215–222.

Gijtenbeek, J.M.M., van den Bent, M.J., Vecht, Ch.J., 1999. Cyclosporine neurotoxicity: a review. J. Neurol. 246, 339–346.

Gimeno, G., Carpentier, P.H., Desquand-Billiald, S., Hanf, R., Finet, M., 1998. L-Arginine and *N*G-nitro-L-arginine methyl ester cause macromolecular extravasation in the microcirculation of awake hamsters. Eur. J. Pharmacol. 346, 275–282.

Grant, D., Kneteman, N., Tchervenkov, J., Roy, A., Murphy, G., Tan, A., Hendricks, L., Guilbault, N., Levy, G., 1999. Peak cyclosporine levels (Cmax) correlate with freedom from liver graft rejection: results of a prospective, randomized comparison of neoral and sandimmune for liver transplantation (NOF-8). Transplantation 67, 1133–1137.

Hayashi, Y., Nomura, M., Yamagishi, S., Harada, S., Yamashita, J., Yamamoto, H., 1997. Induction of various blood–brain barrier properties in non-neural endothelial cells by close apposition to co-cultured astrocytes. Glia 19, 13–26.

Ikesue, H., Kataoka, Y., Kawachi, R., Dohgu, S., Shuto, H., Oishi, R., 2000. Cyclosporine enhances (α_1-adrenoceptor-mediated nitric oxide production in C6 glioma cells. Eur. J. Pharmacol. 407, 221–226.

Isobe, I., Watanabe, T., Yotsuyanagi, T., Hazemoto, N., Yamagata, K., Ueki, T., Nakanishi, K., Asai, K., Kato, T., 1996. Astrocytic contributions to blood–brain barrier (BBB) formation by endothelial cells: a possible use of aortic endothelial cell for in vitro model. Neurochem. Int. 28, 523–533.

Kahan, B.D., 1989. Cyclosporine. N. Engl. J. Med. 321, 1725–1738.

Kahan, B.D., Dunn, J., Fitts, C., Van Buren, D., Wombolt, D., Pollak, R., Carson, R., Alexander, J.W., Choc, M., Wong, R., 1995. Reduced inter- and intrasubject variability in cyclosporine pharmacokinetics in renal transplant recipients treated with a microemulsion formulation in conjunction with fasting, low-fat meals, or high-fat meals. Transplantation 59, 505–511.

Keown, P., Niese, D., 1998. Cyclosporine microemulsion increases drug exposure and reduces acute rejection without incremental toxicity in de novo renal transplantation. International Sandimmun Neoral Study Group. Kidney Int. 54, 938–944.

Kochi, S., Takanaga, H., Matsuo, H., Naito, M., Tsuruo, T., Sawada, Y., 1999. Effect of cyclosporine A or tacrolimus on the function of blood–brain barrier cells. Eur. J. Pharmacol. 372, 287–295.

Kochi, S., Takanaga, H., Matsuo, H., Ohtani, H., Naito, M., Tsuruo, T., Sawada, Y., 2000. Induction of apoptosis in mouse brain capillary endothelial cells by cyclosporin A and tacrolimus. Life Sci. 66, 2255–2260.

Liu, S.M., Sundqvist, T., 1997. Nitric oxide and cGMP regulate endothelial permeability and F-actin distribution in hydrogen peroxide-treated endothelial cells. Exp. Cell Res. 235, 238–244.

Lum, H., Malik, A.B., 1994. Regulation of vascular endothelial barrier function. Am. J. Physiol. 267, L223–L241.

Marks, A.R., 1996. Cellular functions of immunophilins. Physiol. Rev. 76, 631–649.

McCarthy, K.D., de Vellis, J., 1980. Preparation of separate astroglial and oligodendroglial cell cultures from rat cerebral tissue. J. Cell Biol. 85, 890–902.

Menconi, M.J., Unno, N., Smith, M., Aguirre, D.E., Fink, M.P., 1998. Nitric oxide donor-induced hyperpermeability of cultured intestinal epithelial monolayers: role of superoxide radical, hydroxyl radical, and peroxynitrite. Biochem. Biophys. Acta 1425, 189–203.

Nakatsubo, N., Kojima, H., Kikuchi, K., Nagoshi, H., Hirata, Y., Maeda, D., Imai, Y., Irimura, T., Nagano, T., 1998. Direct evidence of nitric oxide production from bovine aortic endothelial cells using new fluorescence indicators: diaminofluoresceins. FEBS Lett. 427, 263–266.

Partridge, W.M., 1999. Blood–brain barrier biology and methodology. J. Neurovirology 5, 556–569.

Pirsch, J.D., Miller, J., Deierhoi, M.H., Vincenti, F., Filo, R.S., 1997. A comparison of tacrolimus (FK506) and cyclosporine for immunosuppression after cadaveric renal transplantation. FK506 kidney transplant study group.. Transplantation 63, 977–983.

Rauh, J., Meyer, J., Beuckmann, C., Galla, H.-J., 1992. Development of an in vitro cell culture system to mimic the blood–brain barrier. Prog. Brain Res. 91, 117–121.

Rubin, L.L., Staddon, J.M., 1999. The cell biology of the blood–brain barrier. Annu. Rev. Neurosci. 22, 11–28.

Sastradipura, D.F., Nakanishi, H., Tsukuba, T., Nishishita, K., Sakai, H., Kato, Y., Gotow, T., Uchiyama, Y., Yamamoto, K., 1998. Identification of cellular compartments involved in processing of cathepsin E in primary cultures of rat microglia. J. Neurochem. 70, 2045–2056.

Schinkel, A.H., 1999. P-glycoprotein, a gatekeeper in the blood–brain barrier. Adv. Drug Deliv. Rev. 5, 179–194.

Shuto, H., Kataoka, Y., Kanaya, A., Matsunaga, K., Sueyasu, M., Oishi, R., 1998. Enhancement of serotonergic neural activity contributes to cyclosporine-induced tremors in mice. Eur. J. Pharmacol. 341, 33–37.

Shuto, H., Kataoka, Y., Fujisaki, K., Nakao, T., Sueyasu, M., Miura, I., Watanabe, Y., Fujiwara, M., Oishi, R., 1999. Inhibition of GABA system involved in cyclosporine-induced convulsions. Life Sci. 65, 879–887.

Tatsuta, T., Naito, M., Oh-hara, T., Sugawara, I., Tsuruo, T., 1992. Functional involvement of P-glycoprotein in blood–brain barrier. J. Biol. Chem. 267, 20383–20391.

Tatsuta, T., Naito, M., Mikami, K., Tsuruo, T., 1994. Enhanced expression by the brain matrix of P-glycoprotein in brain capillary endothelial cells. Cell Growth Differ. 5, 1145–1152.

Terasaki, T., Ohtsuki, S., Hori, S., Takanaga, H., Nakashima, E., Hosoya, K., 2003. New approaches to in vitro models of blood–brain barrier drug transport. Drug Discov. Today 8, 944–954.

Trevin, S., Kataoka, Y., Kawachi, R., Shuto, H., Kumakura, K., Oishi, R., 1998. Direct and continuous electrochemical measurement of noradrenaline-induced nitric oxide production in C6 glioma cells. Cell. Mol. Neurobiol. 18, 453–458.

The U.S. Multicenter FK506 Liver Study Group, 1994. A comparison of tacrolims (FK 506) and cyclosporine for immunosuprresion in liver transplantation. N. Engl. J. Med. 331, 1110–1115.

Verkhratsky, A., Kettenmann, H., 1996. Calciun signaling in gilal cells. Trends Neurosci. 19, 346–352.

Yakel, J.L., 1997. Calcineurin regulation of synaptic function: from ion channels to transmitter release and gene transcription. Trends Pharmacol. Sci. 18, 124–134.

Yamauchi, A., Donghu, S., Naito, M., Tsuruo, T., Sawada, Y., Kai, M., Kataoka, Y. Nitric oxide lowers the function of tight junction and P-glycoprotein at the blood-brain barrier. Cell. Mol. Neurobiol. (in press).

Zhang, X.-D., Morishima, S., Ando-Akatsuka, Y., Takahashi, N., Nabekura, T., Inoue, H., Shimizu, T., Okada, Y., 2004. Expression of novel isoforms of the ClC-1 chloride channel in astrocytic glial cells in vitro. Glia 47, 46–57.

Cellular and Molecular Neurobiology, Vol. 24, No. 5, October 2004 (© 2004)

Tacrolimus-Induced Neurotoxicity and Nephrotoxicity Is Ameliorated by Administration in the Dark Phase in Rats

Atsushi Yamauchi,[1,3] Ryozo Oishi,[2] and Yasufumi Kataoka[1]

Received December 24, 2003; accepted January 9, 2004

SUMMARY

1. Tacrolimus, a potent immunosuppressant, induces impaired renal function and neurological complications. We investigated the influence of dosing time on the neurotoxicity, nephrotoxicity, and immunosuppressive effect of tacrolimus in rats.

2. The repeated injection of tacrolimus in the light phase (8:00) produced a significantly greater increase than that in the dark phase (20:00) in the duration of harmine-induced tremors and in the blood urea nitrogen (BUN) concentration in rats. An immunosuppressive effect of tacrolimus on the xenotransplantation of mouse-to-rat skin grafts was apparent in the dark phase but not in the light phase.

3. The dosing time-dependent pharmacokinetic results were not observed when tacrolimus concentrations in rat whole blood were measured after a single or repeated injection in the light or dark phase.

4. These findings suggest that treatment in the active phase of the diurnal cycle ameliorates neurotoxicity and nephrotoxicity while maintaining the immunosuppressive effect of tacrolimus. The present findings have important implications for therapeutic approaches to avoid tacrolimus-induced neurotoxicity and nephrotoxicity.

KEY WORDS: tacrolimus; neurotoxicity; nephrotoxicity; circadian rhythm; rats.

INTRODUCTION

Tacrolimus is a potent immunosuppressant that blocks calcineurin-mediated T cell activation by binding to immunophilin (FKBP12). This compound is used to prevent allograft rejection in solid organ transplantation and in fatal graft-versus-host diseses after bone marrow transplantation. Multicenter, randomized trials in the USA and Europe demonstrated that tacrolimus induced impaired renal function and neurological complications with a relatively high frequency (20–40%) (European FK506 Multicentre Liver Study Group, 1994; The U.S. Multicenter FK506 Liver Study

[1] Department of Pharmaceutical Care and Health Sciences, Faculty of Pharmaceutical Sciences, Fukuoka University, Nanakuma, Jonan-ku, Fukuoka, Japan.

[2] Department of Hospital Pharmacy, Faculty of Medicine, Kyushu University, Maidashi, Higashi-ku, Fukuoka, Japan.

[3] To whom correspondence should be addressed at Department of Pharmaceutical Care and Health Sciences, Faculty of Pharmaceutical Sciences, Fukuoka University, 8-19-1 Nanakuma, Jonan-ku, Fukuoka, 814-0180, Japan; e-mail: atyama@cis.fukuoka-u.ac.jp.

0272-4340/04/1000-0695/0

Group, 1994). Neurotoxicity including tremors, convulsions, and encephalopathy occurred frequently in patients with high blood concentrations of tacrolimus, although these concentrations were within the therapeutic range. The efficacy or toxicity of drugs such as anticancer drugs has been shown to depend on the dosing time (Levi *et al.*, 1997; Ohdo *et al.*, 2001). Various physiological rhythms in living organisms are considered to be responsible for such chronopharmacological reactions to drugs. Chronotherapy including an optimization of the dosing time is capable of producing more efficient and safer prescriptions for patients than conventional therapy.

The mechanisms of neurotoxicity and nephrotoxicity of tacrolimus are not fully understood. On the basis of our findings plus several reports concerning cyclosporine, an immunosuppressive agents, we present the notion that the immunophilin ligands exert neurotoxicity because of an inhibition of γ-aminobutyric acid neurotransmission and an activation of serotonergic neural activity and nitric oxide production (Fujisaki *et al.*, 2002; Ikesue *et al.*, 2000; Shuto *et al.*, 1998, 1999; Snyder *et al.*, 1998; Steiner *et al.*, 1996; Tominaga *et al.*, 2001;). Several bioactive substances including renine, endothelins, transforming growth factor-β, and nitric oxide are involved in the nephrotoxicity induced by cyclosporin and tacrolimus (Bobadilla *et al.*, 1998; Isram *et al.*, 2001; Kupferman *et al.*, 1994; Lanese *et al.*, 1994; Lanese and Conger, 1993). The physiological activities of these various substances in the brain or kidney are known to indicate circadian rhythms (Brandenberger *et al.*, 1994; Cardinali *et al.*, 1998; Hutson *et al.*, 1984; Hwang *et al.*, 1998). It is, therefore, likely that the incidence of adverse reactions to tacrolimus shows dosing time-dependent variations.

In the present study, we investigated the influence of subchronic treatment with tacrolimus in the light or dark phase of a day for 1–2 weeks on the occurrence of harmine-induced tremors and renal dysfunction in rats. The dosing time-dependent immunosuppressive effect of tacrolimus was also examined using a mouse-to-rat xenotransplantation model. To test whether pharmacokinetic factors are involved in the chronopharmacological action of tacrolimus, the amounts of tacrolimus in rat whole blood were assessed at various periods after a single or subchronic injection in the light or dark phase.

MATERIALS AND METHODS

Animals

Male Wistar rats (7 weeks old) were purchased from Kyudo (Saga, Japan). The animals were maintained on a 12 h light/dark schedule (lights on 7:00 A.M.) at a temperature of 23 ± 2°C with free access to food and water. They were adapted to the light/dark cycle for 2 weeks before the experiments. All the procedures involving experimental animals adhered to the law (No. 105) and notification (No. 6) of the Japanese Government, and were approved by the Laboratory Animal Care and Use Committee of Fukuoka University.

Drugs

Tacrolimus (prograf® injection: Fujisawa Pharmaceutical, Osaka, Japan) was diluted with saline immediately before use. The vehicle solution for the control consisted of polyoxyethylene castor oil (Cremophor EL®, Sigma Chemical CO., St. Louis, MO), ethanol (Wako Pure Chemical Industries Ltd., Osaka, Japan), and saline. This composition was the same as that for the Prograf® injection. Harmine hydrochloride (Sigma Chemical CO., St. Louis, MO) was dissolved in saline. Tacrolimus, vehicle, and harmine were injected intraperitoneally (i.p.) in a volume of 0.5, 0.5, and 0.1 mL/100 g body weight, respectively.

Influence of the Dosing Time of Tacrolimus on Harmine-Induced Tremors and the Concentrations of Serum BUN and Creatinine

Effects of tacrolimus on harmine-induced tremors were evaluated as previously described (Shuto *et al.*, 1998). Tacrolimus (2 mg/kg) or vehicle was injected i.p. once a day for 7 days at 8:00 for the light group or 20:00 for the dark group. Each rat was placed in a screened cage (21.5 × 32× 14 cm) immediately after the 7th injection of tacrolimus to allow adaptation to the new environment and then was introduced to the tremor test. Harmine (10 mg/kg i.p.) was injected 55 min after the final tacrolimus injection. The summed duration of harmine-induced tremors was measured during the 15-min period from 5 to 20 min after harmine administration by the same observer blinded to the pretreatment with tacrolimus or vehicle.

To determine the serum creatinine and BUN concentrations with a Vision analyzer (Abbot Laboratories, Abbot Park, III), blood samples were collected from the rat tail vein 24 h after the final chronic treatment (once a day for 14 days) with tacrolimus (2 mg/kg i.p.) or vehicle at 8:00 or 20:00.

Influence of the Dosing Time of Tacrolimus on Xenograft Survival in Rats Following Xenotransplantation of a Mouse-To-Rat Skin Graft

To make the xenotransplantation model of the mouse-to-rat skin graft, Wistar rats and C57BL/6J mice (15–20 g) were employed as recipients and donors, respectively. The animals were operated on under sodium pentobarbital anesthesia. A square piece (1 cm^2) of skin obtained from the back of the donor mouse was transplanted to where the skin (1 cm^2) was removed from the back of the recipient rat. The skin grafts were protected by gauze with gentacin ointment and bandages for 6 days and rats were housed individually (Shapira *et al.*, 1999).

Xenotransplantation was performed immediately after the first injection of tacrolimus (2 mg/kg i.p.) or vehicle at 8:00 (light group) or 20:00 (dark group). The duration of xenograft survival was determined in each rat with the repeated injection of tacrolimus or vehicle (once a day at 8:00 or 20:00). Rejection was defined as a complete separation of the graft (Shapira *et al.*, 1999).